Potentiation in mouse lumbrical muscle without myosin light chain phosphorylation: Is resting calcium responsible?

Ian C. Smith,[1] William Gittings,[2] Jian Huang,[3] Elliott M. McMillan,[1] Joe Quadrilatero,[1] A. Russell Tupling,[1] and Rene Vandenboom[2]

[1]Department of Kinesiology, University of Waterloo, Waterloo, Ontario N2L 3G1, Canada
[2]Center for Bone and Muscle Health, Brock University, St. Catharines, Ontario L2S 3A1, Canada
[3]Department of Physiology, University of Texas Southwestern Medical Center, Dallas, TX 75390

The increase in isometric twitch force observed in fast-twitch rodent muscles during or after activity, known universally as potentiation, is normally associated with myosin regulatory light chain (RLC) phosphorylation. Interestingly, fast muscles from mice devoid of detectable skeletal myosin light chain kinase (skMLCK) retain a reduced ability to potentiate twitch force, indicating the presence of a secondary origin for this characteristic feature of the fast muscle phenotype. The purpose of this study was to assess changes in intracellular cytosolic free Ca^{2+} concentration ($[Ca^{2+}]_i$) after a potentiating stimulus in mouse lumbrical muscle (37°C). Lumbricals were loaded with the Ca^{2+}-sensitive fluorescent indicators fura-2 or furaptra to detect changes in resting and peak, respectively, intracellular Ca^{2+} levels caused by 2.5 s of 20-Hz stimulation. Although this protocol produced an immediate increase in twitch force of 17 ± 3% (all data are $n = 10$) ($P < 0.01$), this potentiation dissipated quickly and was absent 30 s afterward. Fura-2 fluorescence signals at rest were increased by 11.1 ± 1.3% ($P < 0.01$) during potentiation, indicating a significant increase in resting $[Ca^{2+}]_i$. Interestingly, furaptra signals showed no change to either the amplitude or the duration of the intracellular Ca^{2+} transients (ICTs) that triggered potentiated twitches during this time ($P < 0.50$). Immunofluorescence work showed that 77% of lumbrical fibers expressed myosin heavy chain isoform IIx and/or IIb, but with low expression of skMLCK and high expression of myosin phosphatase targeting subunit 2. As a result, lumbrical muscles displayed no detectable RLC phosphorylation either at rest or after stimulation. We conclude that stimulation-induced elevations in resting $[Ca^{2+}]_i$, in the absence of change in the ICT, are responsible for a small-magnitude, short-lived potentiation of isometric twitch force. If operative in other fast-twitch muscles, this mechanism may complement the potentiating influence of myosin RLC phosphorylation.

The Journal of General Physiology

INTRODUCTION

Excitation–contraction coupling (ECC) of vertebrate striated muscle is the process by which changes in membrane potential are translated into mechanical force by contractile proteins (Gordon et al., 2000). Seminal work by Ebashi and Endo (1968) established that calcium release from the sarcoplasmic reticulum with subsequent binding of Ca^{2+} ion to regulatory proteins resident on the thin filament was the key intermediate step in this process. Subsequent work has provided evidence that the activation of the contractile apparatus, and resultant force, work, and power, is a complex process involving both Ca^{2+}-dependent and Ca^{2+}-independent activation of the thin filament, including several inter- and intrafilament cooperative interactions (Lehrer, 2011).

During ECC, muscle force may be modulated via changes in the amplitude of the Ca^{2+} signal delivered to the contractile apparatus or by the Ca^{2+} sensitivity of the contractile apparatus. In this simple two-compartment model, an augmented Ca^{2+} signal may be achieved via an augmented release from the voltage-sensitive Ca^{2+} release channels or reduced Ca^{2+} buffering such as that performed via the sarcoplasmic–endoplasmic reticulum Ca^{2+} ATPase pumps, either of which could potentiate twitch contractions by increasing the Ca^{2+} occupancy of TnC and thus increasing the probability of "open" states on the regulated thin filament (McKillop and Geeves, 1993; Maytum et al., 1999). An increased Ca^{2+} sensitivity, on the other hand, may be mediated at the level of the myofilaments by muscle length and attendant variations in myofilament interdistance, as first demonstrated by Endo (1972) in skinned and later confirmed by Claflin et al. (1998) in intact skeletal fibers. In addition to these geometric factors, posttranslational modifications of contractile proteins, such as the phosphorylation of the myosin regulatory light chains

Correspondence to Rene Vandenboom: rvandenboom@brocku.ca

Abbreviations used in this paper: AM, acetoxymethyl; $[Ca^{2+}]_i$, intracellular cytosolic free Ca^{2+} concentration; ECC, excitation–contraction coupling; EDL, extensor digitorum longus; ICT, intracellular Ca^{2+} transient; MHC, myosin heavy chain; MYPT2, myosin phosphatase targeting subunit 2; PS, potentiating stimulus; RLC, regulatory light chain; skMLCK, skeletal myosin light chain kinase.

The Rockefeller University Press $30.00
J. Gen. Physiol. Vol. 141 No. 3 297–308
www.jgp.org/cgi/doi/10.1085/jgp.201210918

(RLCs), have been demonstrated to increase the Ca^{2+} sensitivity of both skeletal and cardiac muscle cells (Persechini et al., 1985; Sweeney and Kushmerick, 1985; Sweeney and Stull, 1986). Thus, it seems clear that the ECC process of vertebrate striated muscle is subject to myriad influences that modulate the Ca^{2+} response of the myofilament assembly.

Close and Hoh (1968) were among the first to propose that stimulation-induced alterations to ECC could account for a classical characteristic of the mammalian fast-twitch muscle phenotype, that of posttetanic potentiation, defined as the increase in isometric twitch force observed after brief tetanic stimulation. In this regard, studies using isolated fast-twitch rodent skeletal muscle have shown quantitative associations between phosphorylation of the RLC and isometric twitch force potentiation (Klug et al., 1982; Manning and Stull, 1982; Moore and Stull, 1984; Vandenboom et al., 1997). Indeed, more recent studies using mouse extensor digitorum longus (EDL) muscle devoid of the enzymatic apparatus for phosphorylating the RLC show that, although posttetanic potentiation is completely absent, staircase potentiation, the gradual increase noted in isometric twitch force during low frequency stimulation, was still evident albeit reduced compared with wild-type responses (Zhi et al., 2005; Gittings et al., 2011). Thus, although a universal mechanism is often assumed, evidence exists to suggest that alterations in the Ca^{2+} signal delivered to the myofilament proteins may account for some aspects of potentiation phenomena. This conclusion is in fact consistent with results from rat hind limb disuse models demonstrating staircase potentiation when RLC phosphorylation is absent or reduced (Rassier et al., 1999; MacIntosh et al., 2008).

Although a myosin RLC phosphorylation-mediated increase in the Ca^{2+} sensitivity of force development may be the prevalent mechanism, few studies have examined the contribution of altered Ca^{2+} signals on twitch force potentiation. Thus, the purpose of this study was to assess how stimulation-induced alterations to ECC may contribute to potentiation using the mouse lumbrical muscle model (in vitro at 37°C). To this end, lumbrical muscles were loaded with either a high or low affinity Ca^{2+}-sensitive fluorescent indicator to determine resting and peak intracellular cytosolic free Ca^{2+} concentration ($[Ca^{2+}]_i$), respectively, before and after a tetanic stimulus that potentiated the twitch contractions. We hypothesized that the mechanism for this persistent twitch force potentiation is the influence of repetitive stimulation on either resting or peak $[Ca^{2+}]_i$. Immunofluorescence and immunohistochemical characterization of the mouse lumbrical provide a comprehensive model with far-reaching implications for understanding this fundamental property of mammalian fast-twitch skeletal muscle.

MATERIALS AND METHODS

All procedures used in this study received ethical approval from the University of Waterloo Committee for Animal Care as well as from the Brock University Animal Care and Use Committee. The basic methods and procedure for obtaining and mounting lumbrical muscles were based on those described by Claflin and Brooks (2008). Adult male C57BL/6 mice (28.0 ± 0.6 g) (The Jackson Laboratory) were killed by cervical dislocation, after which the hind paws were removed and placed in a dish containing a Tyrode's dissecting solution (mM: 136.5 NaCl, 5.0 KCl, 11.9 $NaHCO_3$, 1.8 $CaCl_2$, 0.40 NaH_2PO_4, 0.10 EDTA, and 0.50 $MgCl_2$, pH 7.5; on ice), and the lumbrical muscles from both hind paws were subsequently removed. Isolated muscles were suspended horizontally between the arms of a high speed length controller (model 322C; Aurora Scientific Inc.) and a force transducer (model 400A; Aurora Scientific Inc.) while immersed in an oxygenated Tyrode's experimental solution (mM: 121.0 NaCl, 5.0 KCl,

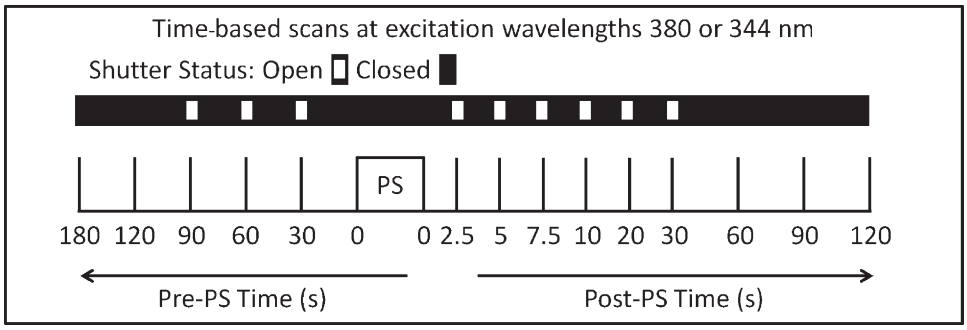

Figure 1. Scheme showing stimulation protocol and fluorescent ratio measurements. The experimental protocol for simultaneous collection of mechanical and fluorescent light data from lumbricals is shown. Muscles were loaded with either a high or a low affinity Ca^{2+}-sensitive fluorescent indictor (fura-2 and furaptra, respectively) before the start of these procedures; thus, all contractile data were obtained from muscles loaded with indicator dye. The scheme shows the timing of shutter opening and closing; each twitch (marked as a vertical line) was framed by a 1-s window of excitation light. This minimized exposure to UV light and thus the loss of light signal during each experiment. Within each experiment, four to five runs of the protocol were conducted, and fluorescent signals from all runs were averaged for formation of representative ratio signals for resting and peak (fura-2 and furaptra, respectively). Because each muscle was only loaded with one of the dyes, the derivation of resting and of peak Ca^{2+} intracellular concentrations ($[Ca^{2+}]_i$) always came from different muscles. In each case, and regardless of the dye, the experiment was terminated when the signal to noise ratio was deemed insufficient. In most cases, the protocol was repeated four times per muscle. Note that the last twitch in the post-PS period occurred 30 s before the first pre-PS twitch in the next sequence. In most muscles, each sequence of 380- and 344-nm excitation was alternated eight times, producing four ratio signals (380/344 nm) per twitch per muscle. PS, potentiating stimulus.

24.0 $NaHCO_3$, 1.8 $CaCl_2$, 0.40 NaH_2PO, 5.50 glucose, 0.10 EDTA, and 0.50 $MgCl_2$, pH 7.3). Based on the binding affinity of EDTA to the constituent metal ions, free concentrations of Ca^{2+} and Mg^{2+} were estimated at 1.7 and 0.5 mM, respectively, in the Tyrode's solutions. Bath temperature was maintained at 37°C throughout the experiment. 0.2-ms stimulus pulses were delivered via imbedded platinum plate field stimulus electrodes using a stimulator (model 701C; Aurora Scientific Inc.). The stimulus voltage at which twitch force plateaued was found and then increased to 1.25 times this level for the duration of each experiment on each muscle. After a 15-min equilibration period, muscles were set to optimal length (L_o) for isometric twitch force development using a software-controlled procedure. Force data were collected online at 10,000 Hz and stored for analysis. Emitted fluorescence signals were collected by a microscope photometer system (D-104; Photon Technology International) affixed with photomultiplier tubes (PMTs; model 814; Photon Technology International) in analogue mode at 10,000 Hz and stored for subsequent analysis.

Experimental model and protocol

The mouse lumbrical muscle model has been used previously to study ECC (e.g., Månsson et al., 1989; Wang and Kerrick, 2002; Claflin and Brooks, 2008). A key advantage is that, in addition to providing a stable preparation for study at high temperatures (Barclay, 2005), the small size of the lumbrical makes it highly amenable to loading with membrane-permeant acetoxymethyl (AM) forms of dyes. The principal measurements of $[Ca^{2+}]_i$ reported in this study were made using the excitation-shifted ratioable fluorescent indicators furaptra and fura-2, although a subset of experiments was performed using the emission-shifted ratioable fluorescent indicator indo-1 (Molecular Probes). Loading of AM-furaptra or AM–fura-2 was accomplished by soaking mounted muscles in ~1 ml Tyrode's experimental solution containing 20 µM dye for 60 min at 32°C, replacing the solution after 30 min. After 60 min of loading, the dye-containing solution was washed out several times and ultimately replaced with normal Tyrode's experimental solution, and the temperature was raised to 37°C. Background fluorescence was obtained before and after loading to verify adequate dye loading and to control for the contribution of autofluorescence to records (i.e., subtracted from all subsequent records).

The timeline and experimental procedure for assessing $[Ca^{2+}]_i$ during potentiation is shown schematically in Fig. 1. After dye loading and preliminary procedures were completed, the muscles received a single stimulus pulse every 30 s until a steady-state isometric twitch force was repeatedly observed. The fluorescence ratio representing resting or peak $[Ca^{2+}]_i$ in the unpotentiated state was obtained from the last three twitches in this series. The regular interval of stimulus pacing was then stopped, and a potentiating stimulus (PS) consisting of 20 Hz for 2.5 s was applied. Thereafter, all muscles received single stimulus pulses to elicit potentiated twitches at 2.5, 5, 7.5, 10, 20, and 30 s after PS. Additional twitches were elicited at 30-s intervals over the next 3 min, a time sufficient to dissipate all potentiation before the protocol was repeated. Each of these repeat sequences took ~5 min to complete and were performed eight times per muscle.

Fluorescent data collection

The excitation and emission light path for the main set of experiments is shown in Fig. 2. The muscle chamber was mounted on the stage of an inverted microscope (Axiovert 200; Carl Zeiss)

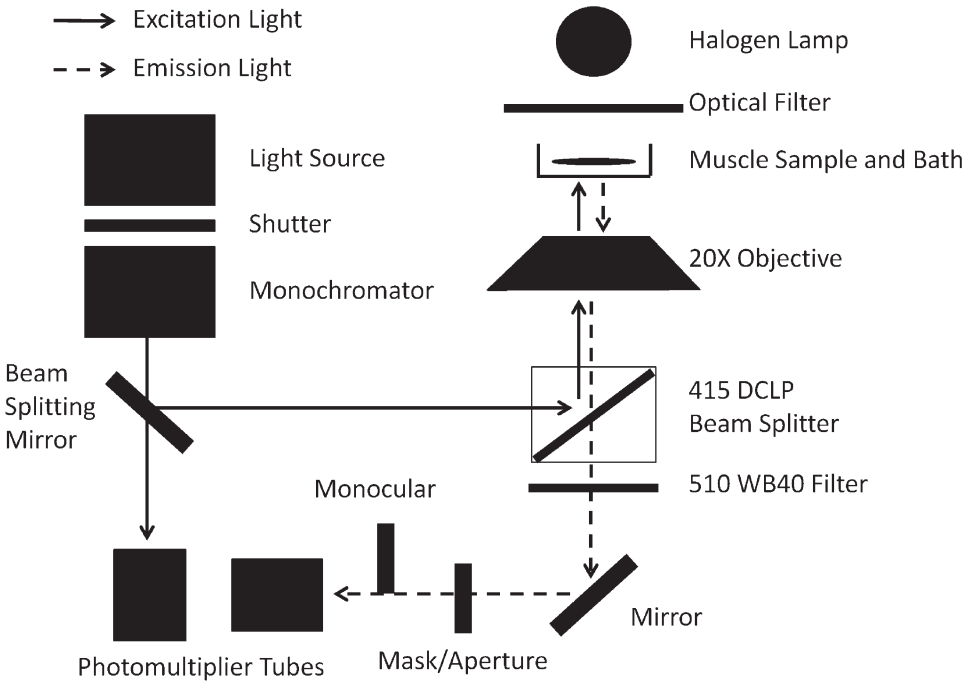

Figure 2. Optical path for excitation and emission light during experiments with fura-2 and furaptra. During experiments with excitation-shifted dyes, the monochromator sent out excitation light at 344 and 380 nm for both fura-2 and furaptra to illuminate the muscle and excite dye fluorescence during isometric twitch contractions. In all cases, slit width was 0.5 mm. Excitation light was deflected by the dichroic beam splitter through the objective and onto the muscle. Emitted light was collected by the objective and passed through the dichroic beam splitter and through an emission filter before being bent 90° by a mirror and directed toward the photomultiplier tube for detection. The mask or aperture was adjusted to focus on a section of the muscle with minimum vertical or lateral movement; thus, mask area did not leave the muscle at any time during contraction. Lumbrical length and width were ~4.0 × 0.6 mm, respectively, and mask size was 0.7 × 0.3 mm, which was large enough to accommodate light emission from 10–12 individual surface muscle fibers.

fitted with a 20× objective (NA of 0.40 and WD of 1.5 mm; LD Plan-Neofluar; Carl Zeiss). Excitation light from the monochromator (Photon Technology International) was deflected by a dichroic beam splitter (415 nm; DCLP; Omega Optical, Inc.) housed in a filter cube in the base of the microscope before being focused on the muscle via the objective. Fluorescent light emitted from the muscle was collected by the objective and passed through the DCLP to an emission filter (510 nm; WB40; Omega Optical, Inc.) before deflection toward and detection by a PMT housed within a detection system (D-104; Photon Technology International). The analogue mode was used for all experiments, and the PMT was set to 600–800-V gain with a time constant of 0.5 ms for furaptra and 5.0 ms for fura-2. Excitation light was monitored in each experiment via a beam-splitting mirror housed within the monochromator, collected using a PMT and stored for later correction of variability of the excitation light caused by room vibrations and/or electrical instabilities.

Fluorescent dye properties

Each of the excitation- and emission-shifted dyes used in these experiments has been widely used to study $[Ca^{2+}]_i$ in both amphibian and mammalian muscle fibers (Konishi et al., 1991, 1993; Westerblad and Allen, 1993; Claflin et al., 1994; Hollingworth et al., 1996, 2012; Morgan et al., 1997; Zhao et al., 1997; Vandenboom et al., 1998; Baylor and Hollingworth, 2003, 2012). Although both furaptra and fura-2 share the same chromophore, i.e., excitation at 344 and/or 380 nm and emission at 510 nm, the characteristics of the emitted fluorescence intensity at different $[Ca^{2+}]_i$ vary considerably between these two dye types; fura-2 fluorescence change is most sensitive to low $[Ca^{2+}]_i$, whereas furaptra fluorescence change is most sensitive to higher $[Ca^{2+}]_i$. These properties are reflected by in vitro K_d values of 224 nM and 44 µM, respectively (Grynkiewicz et al., 1985; Raju et al., 1989; Konishi et al., 1991). This feature allows low affinity dyes such as furaptra to precisely track, with high fidelity, the amplitude and dynamics of the intracellular Ca^{2+} transient (ICT) at most temperatures (e.g., Claflin et al., 1994; Baylor and Hollingworth, 2000). On the other hand, our use of fura-loaded lumbricals to track basal $[Ca^{2+}]_i$ avoids the limitations of furaptra for this purpose and provides a comparison point to previous work. The emitted fluorescence characteristics of indo-1 to different $[Ca^{2+}]_i$ resemble that of fura -2 (Westerblad and Allen, 1993). For all dyes, the ratio technique minimizes contamination of the signal of interest by factors such as motion artifact and/or loss of dye or dye signal by bleaching (see Morgan et al., 1997; Baylor and Hollingworth, 2000, 2011). We tested this assumption by applying sinusoidal length changes to muscles during fluorescent light collection and found no evidence of fiber motion in the resulting ratio signals (not depicted).

Myosin phosphorylation

Parallel experiments were performed in which no contractile or fluorescent data were collected to obtain RLC phosphate content of lumbrical muscles in the unpotentiated and potentiated states. Muscles were quick frozen in liquid nitrogen ∼30 s before and 2.5 s after the PS. All samples were stored at −80°C

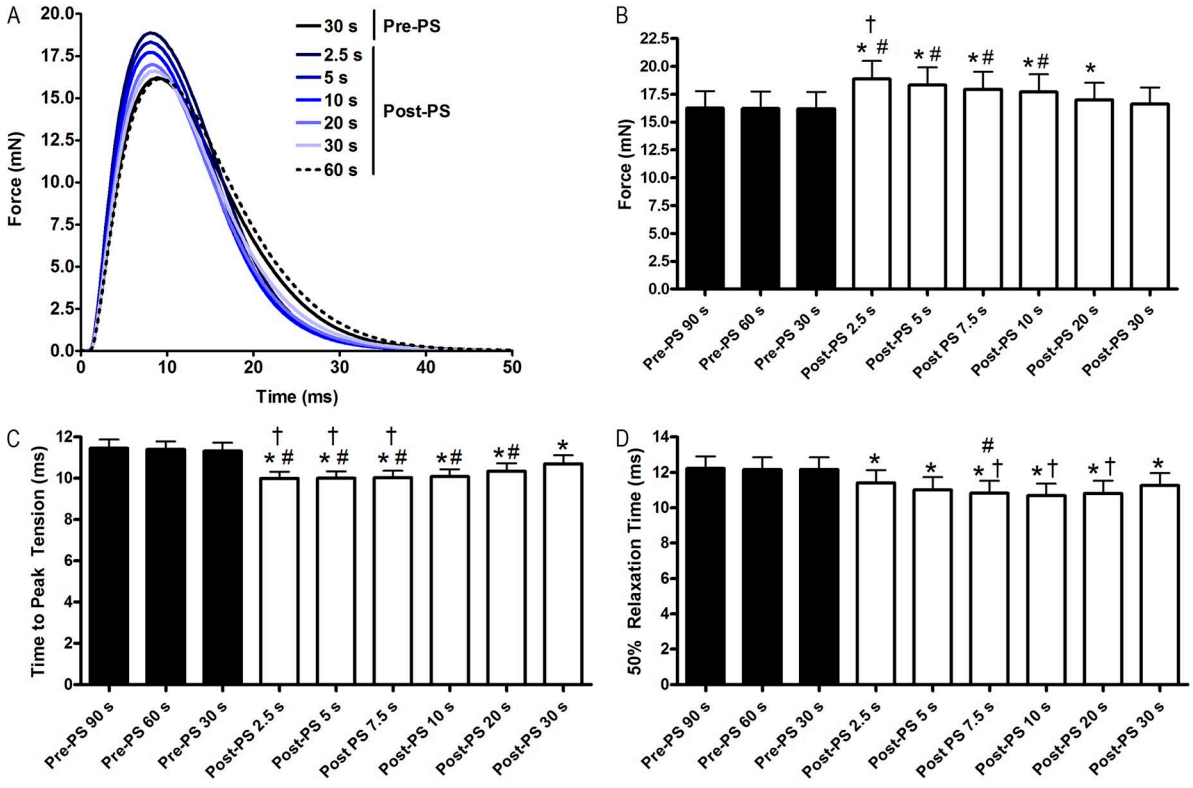

Figure 3. Change in isometric twitch parameters in potentiated lumbrical muscle. (A) Representative twitch force records from one muscle before and up to 60 s after a potentiating stimulation (PS) at 20 Hz for 2.5 s. (B) Peak isometric twitch force pre-PS (closed bars) and up to 30 s post-PS (open bars). *, value is greater than all pre-PS values; †, value is greater than post-PS 7.5, 10, 20, and 30 s; #, value is greater than post-PS 20 and 30 s. (C) Absolute time to peak tension of twitches measured pre-PS and up to 30 s post-PS. *, value is less than all pre-PS values; †, value is less than post-PS 20 s; #, value is less than post-PS 30 s. (D) Absolute half-relaxation time of twitches pre-PS and up to 30 s post-PS. *, value is less than all pre-PS values; †, value is less than post-PS 2.5 s; #, value is less than post-PS 30 s. $P < 0.05$ for B–D.

until they were packed on dry ice and shipped to the laboratory of J. Stull (University of Texas, Southwestern Medical Center, Dallas, TX) for quantification of RLC phosphorylation. Details regarding these methods and procedures have been presented elsewhere (Ryder et al., 2007; Xeni et al., 2011).

MYPT2 and skMLCK content of mouse muscles

Lumbrical, soleus, and EDL muscles were harvested from the mouse hind limb for determination of skeletal myosin light chain kinase (skMLCK) and myosin phosphatase targeting subunit 2 (MYPT2) content as described in Smith et al. (2010). In brief, skMLCK and MYPT2 content was assessed in whole muscle homogenates by Western blot analysis after separation of proteins by electrophoresis using 7.5% polyacrylamide gels and standard SDS/PAGE protocols (Laemmli, 1970). Protein concentrations were determined by the bicinchoninic acid method (Sigma-Aldrich), and Ponceau S (BioShop Canada Inc.) staining was used to control for variation in well loading. Either 8.0 (MYPT2) or 10.0 (skMLCK) µg of total protein was loaded for each muscle sample, with two mice per gel. A linear relationship between band density and protein load for each mouse was established for 2.0–8.0 µg of total protein in soleus for MYPT2 or 2.5–10.0 µg of total protein in EDL for skMLCK. After transfer of proteins to polyvinyl difluoride membranes, MYPT2 was probed using a polyclonal rabbit antibody, whereas skMLCK was probed using a polyclonal goat antibody (provided by J. Stull). Secondary probing was performed with either goat anti–rabbit (MYPT2) or donkey anti–goat (skMLCK) antibodies conjugated with horseradish peroxidase (HRP). Quantification was performed using an HRP substrate detection kit (Luminata; EMD Millipore) and subsequent densitometric analysis (GE Healthcare). MYPT2 content in EDL and lumbrical was expressed relative to soleus, whereas skMLCK content in soleus and lumbrical was expressed relative to EDL, as determined by comparing the band densities to those determined by the generated linear scales at equivalent protein loads.

Fiber typing

Myosin heavy chain (MHC) expression was determined in lumbrical, soleus, and EDL cross sections by immunofluorescence analysis as described by Bloemberg and Quadrilatero (2012). In brief, sections were blocked with 10% goat serum, incubated with primary antibodies against MHC I, MHC IIa, and MHC IIb (Developmental Studies Hybridoma Bank), and then washed in PBS. Sections were then incubated with isotype-specific Alexa Fluor 350 anti–mouse, Alexa Fluor 488 anti–mouse, and Alexa Fluor 555 anti–mouse (Molecular Probes) secondary antibodies, washed in PBS, and mounted with an anti-fade reagent (Prolong Gold; Molecular Probes). This staining procedure allowed for the identification of type I (blue), type IIA (green), type IIB (red), type IIX (unstained), and hybrid (types I/IIA, IIAX, and IIXB) fibers. Type I/IIA hybrid fibers were identified as those staining positively for MHC type I and type IIa. Type IIAX fibers were identified as those staining positive for MHC IIa but at a lower intensity than fibers identified as type IIA. Similarly, fibers were labeled type IIXB if they stained positively for MHC IIb but at a lower intensity than type IIB fibers. Images were captured using a structured illumination fluorescent microscope (Axio Observer Z1) equipped with a camera (AxioCam HRm) and associated software (AxioVision; all from Carl Zeiss).

Statistics

All data are reported as mean ± SEM. Relative changes in mean values for various twitch force and Ca^{2+} parameters were compared by a repeated measures ANOVA followed by Tukey's HSD post-hoc analysis. Differences were considered significant at $P < 0.05$.

RESULTS

We present mechanical, immunofluorescence, and immunohistochemical data that describes a fast-twitch muscle model that appears to be somewhat unique in that isometric twitch force potentiation occurs in the total absence of myosin RLC phosphorylation. Although fast muscles from skMLCK knockout mice display a small amount of potentiation in the absence of stimulation-induced elevations in RLC phosphorylation, lumbrical muscles from wild-type mice appear to mimic this response. Thus, unlike traditional studies performed on wild-type muscles, this attribute of the lumbrical allows for a direct analysis of the contribution of altered $[Ca^{2+}]_i$ to potentiation.

Isometric twitch contractile responses

Representative isometric twitch force records obtained before and after the PS are depicted in Fig. 3 A. These records show how stimulation produced a modest twitch potentiation that dissipated rapidly. Absolute mechanical data characterizing our mouse lumbrical in vitro muscle model are compiled in Table 1, with relative changes to twitch force amplitude and kinetics summarized in

TABLE 1

Twitch parameters before and after a PS in mouse lumbrical muscle at 37°C

Twitch parameter	Pre-PS	Post-PS		Relative change (Post-PS/Pre-PS)	
	−60 s	2.5 s	30 s	2.5 s	30 s
Amplitude (mN)	16.23 ± 1.51	18.87 ± 1.61[a]	16.61 ± 1.50[b]	1.17 ± 0.03[a]	1.03 ± 0.01[b]
Time to peak (ms)	11.39 ± 0.40	10.0 ± 0.32[a]	10.70 ± 0.42[a,b]	0.88 ± 0.01[a]	0.94 ± 0.01[a,b]
1/2 RT (ms)	12.16 ± 0.69	11.41 ± 0.73[a]	11.25 ± 0.72[a]	0.94 ± 0.02[a]	0.92 ± 0.01[a,b]
+dF/dt (mN/ms)	3.41 ± 0.31	4.57 ± 0.42[a]	3.60 ± 0.33[b]	1.34 ± 0.02[a]	1.05 ± 0.01[a,b]
−dF/dt (mN/ms)	−1.14 ± 0.11	−1.40 ± 0.13[a]	−1.23 ± 0.11[a,b]	1.23 ± 0.04[a]	1.08 ± 0.01[a,b]

All data are presented as mean ± SEM ($n = 10$ muscles). Time markers correspond to 60 s before start and 2.5 and 30 s after the PS (20 Hz for 2.5 s). Peak twitch force occurred at 2.5 s after the PS in every muscle examined; all data collected at optimal length for twitch force (L_o). Data corresponds to ICT data presented in Table 2. Amplitude, twitch force from baseline to peak; time to peak, the time for force to rise from baseline to peak; 1/2 RT, time for force to relax from peak to 50% peak; +dF/dt, maximum rate of force production; −dF/dt, maximum rate of force relaxation.

[a]Post-PS value at 2.5 or 30 s significantly different than pre-PS value ($P < 0.05$).

[b]Post-PS value at 30 s significantly different than post-PS value at 2.5 s ($P < 0.05$).

TABLE 2

Intracellular Ca^{2+} at rest and during stimulation in mouse lumbrical muscles at 37°C

Dye and parameter	Time pre-PS	Time post-PS	
Furaptra	−60 s	5.0 s	20 s
Amplitude (Ratio units)	0.0131 ± 0.0007	0.0127 ± 0.0007	0.0132 ± 0.0007
Time to peak (ms)	1.8 ± 0.1	1.8 ± 0.1	1.8 ± 0.1
ICT 50% decay time (ms)	3.1 ± 0.6	2.7 ± 0.4	2.8 ± 0.4
FWHM (ms)	3.6 ± 0.5	3.7 ± 0.4	3.7 ± 0.4
Fura-2	−30 s	2.5 s	30 s
Resting Ca^{2+} (Ratio units)	0.376 ± 0.017	0.418 ± 0.022[a]	0.395 ± 0.019[b]

All data are presented as mean ± SEM (n = 10 furaptra or n = 9 fura-2). Fura-2 data reported for 2.5 and 30 s correspond to peak twitch force potentiation and the first return of peak twitch force to unpotentiated levels after PS, respectively. Furaptra signals during twitch contractions were averages of those occurring 90, 60, and 30 s before the onset of the PS (denoted as −60 s), 2.5, 5.0, and 7.5 s after the end of the PS (denoted as 5.0 s) and 10, 20, and 30 s after the end of the PS (denoted as 20 s) for each muscle. PS, potentiating stimulus (20 Hz for 2.5 s at optimum length for twitch tension (L_o)); ICT, intracellular Ca^{2+} transient; FWHM, full width at half-maximum.

[a]Post-PS value at 2.5 s significantly different than pre-PS value ($P < 0.001$).

[b]Post-PS value at 30 s is significantly different than pre-PS value ($P < 0.01$) and post-PS value at 2.5 s ($P < 0.01$).

Fig. 3 (B–D). The PS produced a maximal increase in isometric twitch force of 17 ± 3% when determined 2.5 s after the cessation of stimulation (n = 10; $P < 0.01$). From this point onwards, potentiation decreased in a monotonic fashion with a halftime of ∼10 s; as a result, twitch force returned to prestimulus unpotentiated levels by 30 s. Along with the elevations in twitch force, twitch time course kinetics were faster and maximal rates of force production and relaxation were higher after the PS (Table 1). Interestingly, these effects were still evident 30 s later, despite the fact that twitch force had returned to pre-PS levels (Table 1); this effect resolved before the subsequent set of contractions. Finally, force returned to baseline in the time period between potentiated twitches (as depicted in the force traces of Figs. 3 and 5), and there was no latent elevation in baseline tension after the PS (not depicted).

Fluorescence measurements

An important limitation of fura-based fluorescence ratio signals is that they cannot provide quantitatively useful data regarding the amplitude or kinetic characteristics of the ICT. By the same token, furaptra-based fluorescence ratio signals cannot be expected to provide quantitatively useful data regarding resting $[Ca^{2+}]_i$ (Baylor and Hollingworth, 2000, 2011). Thus, a complementary approach using both dyes was adopted to provide a more comprehensive picture regarding the influence of prior stimulation on ECC that could account for changes in isometric twitch force and kinetics. Ratio data from all experiments using either fura-2 or furaptra are compiled in Table 2. Averaged fura-2 fluorescence ratio records are shown in Fig. 4 A, with relative changes summarizing all experiments shown in Fig. 4 B. These data clearly show a relatively small but consistent elevation in basal $[Ca^{2+}]_i$ that was highly significant (n = 10; $P < 0.001$) at all potentiation time points. By 30 s after stimulation, the resting fluorescence ratio was still elevated although

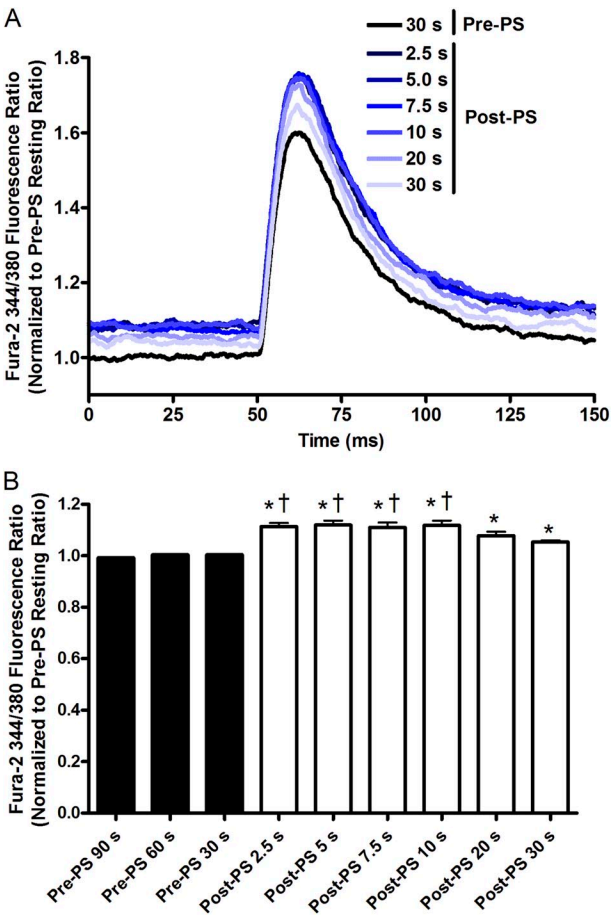

Figure 4. Change in fura-2 fluorescence in potentiated lumbrical muscle. (A) Averaged traces showing unpotentiated (Pre-PS) and potentiated (Post-PS) ICTs. (B) Relative change in the fura-2 344/380-nm emission ratio measured just before the indicated stimulus after a PS of 20 Hz for 2.5 s. *, value is greater than all pre-PS values ($P < 0.001$); †, value is greater than post-PS 30 s ($P < 0.001$). Each trace is the average of nine muscles.

potentiation had dissipated. Resting fluorescence did, however, return to prestimulus (unpotentiated) levels after another 30 s (i.e., within 60 s of completion of the PS). Virtually identical experiments (n = 8) were performed using the indicator indo-1, which has similar Ca^{2+} affinity as fura-2. In these experiments, there was an 8.1 ± 1.3% increase in the resting fluorescence ratio as determined 2.5 s after the PS ($P < 0.001$ vs. prestimulus). This increase dissipated with a similar time course as did the twitch force potentiation, returning to prestimulus levels by 30 s after the PS (not depicted). Thus, the elevation in resting $[Ca^{2+}]_i$ reported by indo-1 fluorescence was quantitatively similar to that reported by fura-2 fluorescence in terms of both magnitude and duration.

Averaged furaptra-based fluorescence ratio signals from identical experiments are shown in Fig. 5, with relative changes for ICT amplitude and full width at half-maximum shown in Table 2, respectively. These data clearly show that, even when measured at the potentiation peak 2.5 s after stimulation, neither the amplitude nor the time course of the ICT was altered relative to the unpotentiated state (n = 10; $P > 0.20$). Although our fura- and furaptra-based fluorescence ratio signals have been analyzed independently of one another, our results indicate that stimulation-induced elevations in resting $[Ca^{2+}]_i$ potentiate isometric twitch force in the complete absence of change to either the amplitude or time course of the subsequent ICT per se.

Myosin RLC phosphorylation, skMLCK, and MYPT2 content

Myosin RLC phosphorylation levels obtained from lumbrical and from EDL muscles are shown in Fig. 6 (A and B). An unexpected result was the complete absence of RLC phosphorylation in lumbrical muscles, as no phosphorylated RLC was detected in samples obtained before or after stimulation. On the other hand, phosphorylated RLC was detected in EDL samples obtained at rest and after stimulation. Consistent with these data was our Western blot analysis showing much lower expression of skMLCK and much higher expression of MYPT2 phosphatase in lumbrical muscle compared with EDL muscle (Fig. 6, C and D). Interesting in this regard was the similarity between soleus and lumbrical levels in both skMLCK and MYPT2 expression.

Fiber-type analysis

Fig. 7 compares the fiber-type composition of lumbrical, EDL, and soleus muscles from adult mice aged 3–5 mo, as determined by immunofluorescence analysis of the myosin isoform (as in Gittings et al., 2011). These data show that the main fiber types contained by adult mouse lumbrical muscle are type IIX and associated hybrids (i.e., type IIAX and type IIXB), comprising ~61% of all fiber types. Notably, only a very small population of type IIB fibers was found. The total fiber count per lumbrical was 302 ± 17 muscle fibers (i.e., ~40% of that in either soleus or EDL).

DISCUSSION

The purpose of this study was to establish if the isometric twitch force potentiation observed in mouse lumbrical muscle could be attributed to stimulation-induced changes in myoplasmic free Ca^{2+} concentration, as opposed to putative increases in Ca^{2+} sensitivity as mediated by RLC phosphorylation. The rationale for this line of inquiry was the presence of potentiation in skMLCK knockout muscles, suggesting at least a minor role for altered ECC in potentiation. By using a fast-twitch muscle that has little or no skMLCK expression (Ryder et al., 2007), we were able to examine potentiation in the absence of the RLC phosphorylation mechanism. The main finding in the present study was the

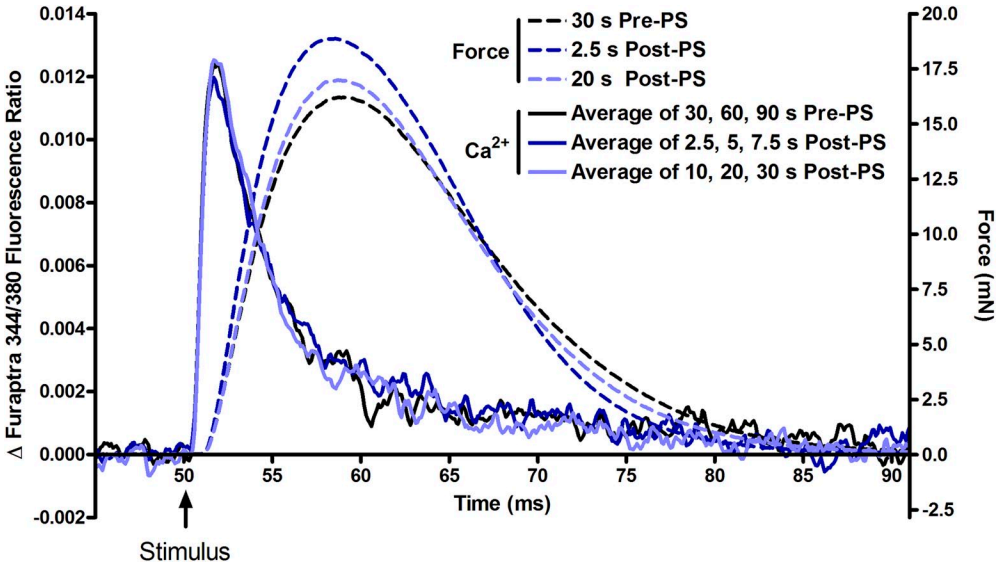

Figure 5. Change in furaptra fluorescence in potentiated lumbrical muscle. Averaged traces showing isometric twitch force and ICTs before and after the PS of 20 Hz for 2.5 s. Each trace is the average of 10 muscles.

presence of a small and rapidly dissipating potentiation temporally correlated with stimulation-induced elevations in resting $[Ca^{2+}]_i$, independent of change to the ICT itself, thus providing evidence for an alternate mechanism for the activity-dependent increases in twitch force often observed in fast-twitch muscle models. Thus, our data suggest the presence of stimulation-induced alterations to Ca^{2+} handling that acutely increases isometric twitch force, a mechanism that may operate independently of the longer term potentiation offered by skMLCK-catalyzed RLC phosphorylation (see Stull et al., 2011).

The mouse lumbrical at 37°C represents a relatively unique model with which to study force potentiation, making it difficult to make direct comparisons of our results with the literature. Although comprised of ~89% of type II fibers, no phosphorylated RLC was detected in our samples either at rest or after stimulation. Although the absence of RLC phosphorylation and the minimal potentiation we observed seems incompatible with the typical rodent fast-twitch muscle profile (Schiaffino and Reggiani, 2011), our Western blot analysis, showing low skMLCK and high MYPT2 phosphatase expression in lumbrical relative to EDL muscle, corroborates the absence of detectable RLC phosphorylation in our experiments. As a general point of comparison, the potentiation of mouse EDL muscle at 35°C reported by Moore et al. (1990) was approximately twice as great in magnitude and duration as we observed. The difference in potentiation between the two studies is perhaps accounted for by the fact that, in their study, stimulation at 5 Hz for 20 s significantly elevated RLC phosphorylation levels. Interesting results from Ryder et al. (2007) may also apply to our experiments. These investigators used transgenic mice overexpressing the skMLCK enzyme in skeletal muscle to show that despite similar levels for RLC phosphorylation (i.e., 50–60% phosphorylated), twitch force potentiation was much greater in EDL than in soleus muscles (Ryder et al., 2007). This apparent uncoupling between RLC phosphorylation and twitch potentiation was hypothesized to be caused by the presence of type I and IIA fibers and the absence of type IIB fibers in soleus relative to EDL muscle; these data thus indicate a strong dependence within species fiber type for the ability of RLC phosphorylation to increase Ca^{2+} sensitivity (Ryder et al., 2007). Indeed,

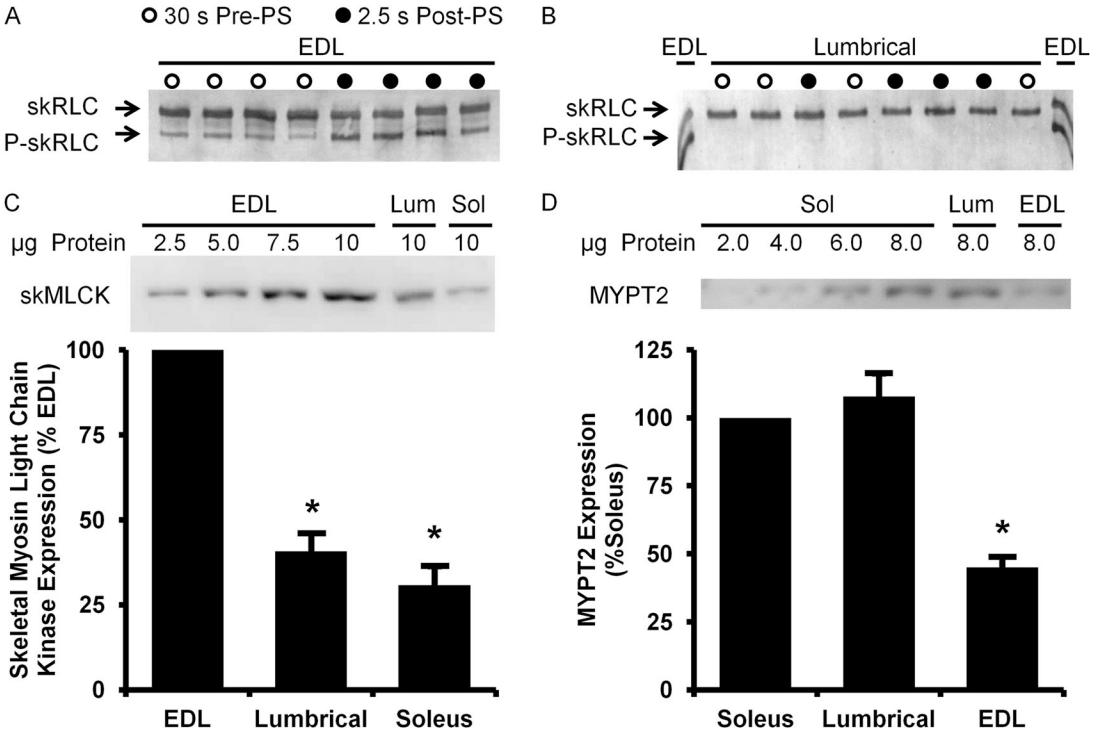

Figure 6. Myosin RLC phosphorylation, skMLCK, and MYPT2 in mouse muscles. Example blots showing phosphorylation levels in skeletal isoforms of myosin RLC (skRLC) in mouse EDL (A) and lumbrical (B) muscle 30 s before and immediately after the PS, revealing stimulation-induced elevations in RLC phosphorylation in EDL but not in lumbrical muscle. (C) Example Western blot and summary data showing skMLCK expression in mouse EDL, lumbrical (Lum), and soleus (Sol) muscle expressed relative to that EDL. *, value different than EDL value ($P < 0.01$; $n = 7$). (D) Example Western blot and summary data showing MYPT2 expression in mouse EDL, lumbrical (Lum), and soleus (Sol) muscle expressed relative to the soleus. *, value different than Sol value ($P < 0.01$; $n = 8$). Notes: For the skMLCK blot, each lane is an individual muscle (i.e., no pooling). For the MYPT2 blot, two lumbricals from the same animal (one from each hind foot) are pooled, whereas soleus and EDL are unpooled (because of size differences). For both skMLCK and MYPT2, each blot had the soleus, EDL, and lumbrical muscle from the same mouse lined up together, with two mice per gel.

our work extends these data by showing that, in the wild-type mouse, skMLCK-catalyzed RLC phosphorylation may be restricted to IIB fibers with little RLC phosphorylation occurring in either IIX or IIA fibers. The relatively minor population of type IIB fibers we found in the lumbrical helps account for the low overall skMLCK expression in this muscle. Moreover, although we could not identify any fiber-type dependence for MYPT2 expression, the relatively high expression of MYPT2 suggests a limited ability to phosphorylate the RLC despite the prevalence of fast fibers.

Putative potentiation mechanism

Any adequate explanation for our results must account for an increased twitch force in the absence of any myosin RLC phosphorylation–mediated increase in Ca^{2+} sensitivity. Although our data does not provide any mechanistic insights, the finding of an unchanged ICT amplitude superimposed upon an elevated basal $[Ca^{2+}]_i$ suggests that the Ca^{2+} activation of the thin filament may have been increased after stimulation. As pointed out by Baylor and Hollingworth (2011), little is known regarding the aftereffects of tetanic stimulation on basal $[Ca^{2+}]_i$. Because this parameter was elevated for as long as potentiation was observed (i.e., 20–30 s) and was reversed shortly thereafter (i.e., 30–60 s), we hypothesize that this change was mechanistically related to twitch force enhancement. One way in which an elevated basal $[Ca^{2+}]_i$ could have directly potentiated twitch force is through an increased binding and, thus, occupancy of the intracellular Ca^{2+} buffer protein parvalbumin in resting muscle. In this hypothesis, although basal $[Ca^{2+}]_i$ was not elevated above the threshold level for force development, partial saturation of parvalbumin-buffering capacity may have increased the fraction of free Ca^{2+} released from the sarcoplasmic reticulum that was able to bind to TnC on the thin filament, an effect not reflected by changes to the ICT itself. Indeed, the increased +dF/dt of potentiated twitches is consistent with an enhanced Ca^{2+} occupancy of TnC at the onset of contraction

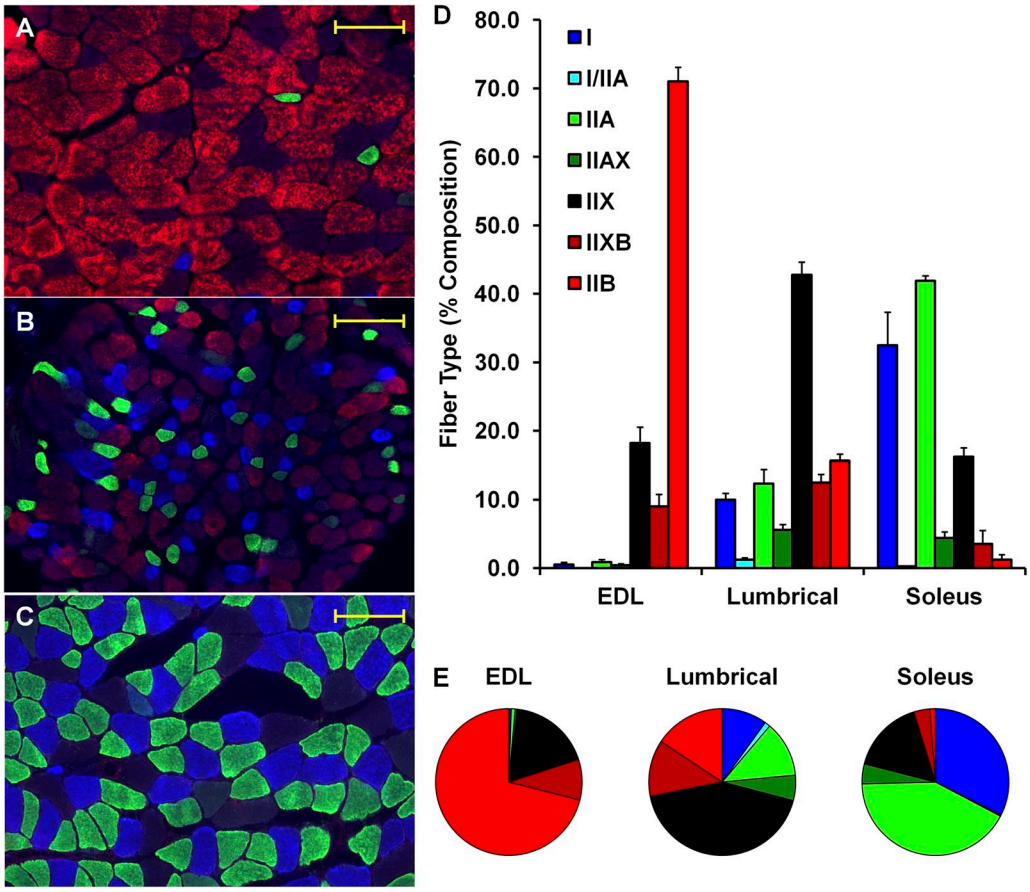

Figure 7. Immunofluorescence analysis of MHC isoform expression of mouse muscles. Example of immunofluorescence staining performed as explained in Materials and methods, showing MHC I (blue), MHC IIa (green), MHC IIx (unstained), and MHC IIb (red) expression patterns in (A) EDL, (B) lumbrical, and (C) soleus muscle. Bars, 100 µm. Fiber-type composition was determined for the entire muscle cross section ($n = 4$ soleus and EDL; $n = 8$ lumbrical), and the data are presented as percent fiber-type composition by muscle in both bar (D) and pie (E) graph form. Note that the variance in fiber cross-sectional areas apparent in A–C is not a function of scaling but a function of muscle of origin, with fiber CSA being smaller in the lumbrical than the EDL, which is in turn smaller than that of the soleus. See also Bloemberg and Quadrilatero (2012).

(Lee et al., 2010). An alternate interpretation of our results is that the increase in basal $[Ca^{2+}]_i$ indirectly potentiated twitch force via some influence on thick filament distribution and/or structure. As an example, Brenner et al. (1982) used permeabilized rabbit psoas skeletal fibers to show the presence of a population of attached but non-force–generating cross-bridges at low ionic strength in the absence of Ca^{2+}. Further to this, Lehrer (2011) has recently proposed the existence of a regulated cross-bridge state that is sensitive to resting or subthreshold levels of $[Ca^{2+}]_i$. Collectively, these studies seem to allow for the possibility that elevations in basal $[Ca^{2+}]_i$ may promote the transition of the attached but pre-force–generating cross-bridge state to the attached and force-generating cross-bridge state during the twitch (Brenner et al., 1982; Lehrer, 2011). A final possibility worth considering is that elevations in basal $[Ca^{2+}]_i$ potentiate twitch force by increasing the occupancy of Ca^{2+}/Mg^{2+}-binding sites located on the RLC (Bagshaw and Reed, 1977; Robertson et al., 1981). Ca^{2+} binding to myosin has been shown to disorganize myosin head position on the thick filament surface of scallop muscle (e.g., Zhao and Craig, 2003, 2008). If this effect of ligand binding to the myosin RLC has the same effect on thin filament–regulated vertebrate skeletal muscle as it does for thick filament–regulated molluscan muscle, it may facilitate the ability of cycling cross-bridges to attain force-generating states (Diffee et al., 1995, 1996). Thus, although our data cannot rule out alternate mechanisms related to changes in metabolites brought about by stimulation (e.g., P_i) (Barclay, 1992), they may be adequately accounted for by the influence of altered basal Ca^{2+} homeostasis in resting muscle on cross-bridge structure and/or distribution.

Relation to previous studies

Decostre et al. (2000) tracked fluorescence signals from the surface of mouse EDL muscles loaded with fura -2 (20°C) during posttetanic potentiation. These investigators observed an ∼10% increase in isometric twitch force immediately after stimulation at 125 Hz for 1 s, a potentiation that then decayed slowly and was absent 300 s later. Consistent with our results, however, elevations in basal and peak $[Ca^{2+}]_i$ were observed, although the absolute change in ICT amplitude was similar in potentiated versus unpotentiated states (Decostre et al., 2000). Interestingly, the application of 1 µM adrenaline to maintain post-stimulus elevations in myosin RLC phosphate content produced a greater and more prolonged potentiation of twitch force (10–15% for >300 s) that was evident after the stimulation-induced alterations in $[Ca^{2+}]_i$ had been reversed. This outcome suggests that, although stimulation-induced elevations in $[Ca^{2+}]_i$ may contribute, they are not a requisite for twitch force potentiation. This helps account for why rat fast-twitch muscle models displaying reduced RLC phosphorylation also exhibit reduced potentiation (Tubman et al., 1996, 1997). Based on these and the present results, stimulation-induced elevations in resting $[Ca^{2+}]_i$ and in RLC phosphorylation may provide an acute and persistent twitch force potentiation, reversed by the rapid return of resting Ca^{2+} homeostasis and/or the slow rate of RLC dephosphorylation by PP1 phosphatase activity, respectively (Stull et al., 2011).

Study limitations

The advantages and disadvantages of using high and low Ca^{2+} affinity indicators for determination of $[Ca^{2+}]_i$ in intact skeletal fibers have recently been presented by Baylor and Hollingworth (2011). Although use of AM dyes offers many advantages, an intractable issue is that of a noncytosolic-specific compartment component to the global fluorescent signal (see Morgan et al., 1997). Thus, although we have assumed that the loci for the elevated resting $[Ca^{2+}]_i$ was the myoplasm, this cannot be absolutely confirmed from the present experiments. In addition, although furaptra retains the ability to precisely track the ICT in the range of 28 to 35°C (Hollingworth et al., 1996), it is possible that the high temperature we used may have mitigated our ability to detect changes in ICT duration caused by the PS.

Summary

Our results provide a putative mechanism for posttetanic potentiation of isometric twitch force reported in the absence of myosin RLC phosphorylation. Although the skMLCK-catalyzed phosphorylation of the myosin RLC should still be considered the primary mechanism, repetitive or high frequency stimulation that elevates resting $[Ca^{2+}]_i$ may contribute a fast-acting component to isometric twitch force potentiation, reversed by the rapid return of Ca^{2+} homeostasis after stimulation. The functional implications of this mechanism remain to be determined.

We would like to thank Dr. Jim Stull for analysis of myosin light chain phosphorylation.

This study was supported by funds provided by the Natural Sciences and Engineering Research Council of Canada (to A.R. Tupling and R. Vandenboom). The authors declare that they do not have any conflicting interests regarding the findings or interpretations of this manuscript.

Angus C. Nairn served as editor.

Submitted: 22 October 2012
Accepted: 17 January 2013

REFERENCES

Bagshaw, C.R., and G.H. Reed. 1977. The significance of the slow dissociation of divalent metal ions from myosin 'regulatory' light chains. *FEBS Lett.* 81:386–390. http://dx.doi.org/10.1016/0014-5793(77)80560-7

Barclay, C.J. 1992. Effect of fatigue on rate of isometric force development in mouse fast- and slow-twitch muscles. *Am. J. Physiol.* 263:C1065–C1072.

Barclay, C.J. 2005. Modelling diffusive O_2 supply to isolated preparations of mammalian skeletal and cardiac muscle. *J. Muscle Res. Cell Motil.* 26:225–235. http://dx.doi.org/10.1007/s10974-005-9013-x

Baylor, S.M., and S. Hollingworth. 2000. Measurement and interpretation of cytoplasmic calcium levels. *News Physiol. Sci.* 15:19–26.

Baylor, S.M., and S. Hollingworth. 2003. Sarcoplasmic reticulum calcium release compared in slow-twitch and fast-twitch fibres of mouse muscle. *J. Physiol.* 551:125–138. http://dx.doi.org/10.1113/jphysiol.2003.041608

Baylor, S.M., and S. Hollingworth. 2011. Calcium indicators and calcium signalling in skeletal muscle fibres during excitation-contraction coupling. *Prog. Biophys. Mol. Biol.* 105:162–179. http://dx.doi.org/10.1016/j.pbiomolbio.2010.06.001

Baylor, S.M., and S. Hollingworth. 2012. Intracellular calcium movements during excitation–contraction coupling in mammalian slow-twitch and fast-twitch muscle fibers. *J. Gen. Physiol.* 139:261–272. http://dx.doi.org/10.1085/jgp.201210773

Bloemberg, D., and J. Quadrilatero. 2012. Rapid determination of myosin heavy chain expression in rat, mouse, and human skeletal muscle using multicolor immunofluorescence analysis. *PLoS ONE.* 7:e35273. http://dx.doi.org/10.1371/journal.pone.0035273

Brenner, B., M. Schoenberg, J.M. Chalovich, L.E. Greene, and E. Eisenberg. 1982. Evidence for cross-bridge attachment in relaxed muscle at low ionic strength. *Proc. Natl. Acad. Sci. USA.* 79:7288–7291. http://dx.doi.org/10.1073/pnas.79.23.7288

Claflin, D.R., and S.V. Brooks. 2008. Direct observation of failing fibers in muscles of dystrophic mice provides mechanistic insight into muscular dystrophy. *Am. J. Physiol. Cell Physiol.* 294:C651–C658. http://dx.doi.org/10.1152/ajpcell.00244.2007

Claflin, D.R., D.L. Morgan, D.G. Stephenson, and F.J. Julian. 1994. The intracellular Ca^{2+} transient and tension in frog skeletal muscle fibres measured with high temporal resolution. *J. Physiol.* 475: 319–325.

Claflin, D.R., D.L. Morgan, and F.J. Julian. 1998. The effect of length on the relationship between tension and intracellular [Ca^{2+}] in intact frog skeletal muscle fibres. *J. Physiol.* 508:179–186. http://dx.doi.org/10.1111/j.1469-7793.1998.179br.x

Close, R., and J.F. Hoh. 1968. The after-effects of repetitive stimulation on the isometric twitch contraction of rat fast skeletal muscle. *J. Physiol.* 197:461–477.

Decostre, V., J.M. Gillis, and P. Gailly. 2000. Effect of adrenaline on the post-tetanic potentiation in mouse skeletal muscle. *J. Muscle Res. Cell Motil.* 21:247–254. http://dx.doi.org/10.1023/A:1005685900196

Diffee, G.M., M.L. Greaser, F.C. Reinach, and R.L. Moss. 1995. Effects of a non-divalent cation binding mutant of myosin regulatory light chain on tension generation in skinned skeletal muscle fibers. *Biophys. J.* 68:1443–1452. http://dx.doi.org/10.1016/S0006-3495(95)80317-6

Diffee, G.M., J.R. Patel, F.C. Reinach, M.L. Greaser, and R.L. Moss. 1996. Altered kinetics of contraction in skeletal muscle fibers containing a mutant myosin regulatory light chain with reduced divalent cation binding. *Biophys. J.* 71:341–350. http://dx.doi.org/10.1016/S0006-3495(96)79231-7

Ebashi, S., and M. Endo. 1968. Calcium ion and muscle contraction. *Prog. Biophys. Mol. Biol.* 18:123–183. http://dx.doi.org/10.1016/0079-6107(68)90023-0

Endo, M. 1972. Stretch-induced increase in activation of skinned muscle fibres by calcium. *Nat. New Biol.* 237:211–213.

Gittings, W., J. Huang, I. Smith, J. Quadrilatero, and R. Vandenboom. 2011. The effect of skeletal myosin light chain kinase gene ablation on the fatigability of mouse fast muscle. *J. Muscle Res. Cell Motil.* 31:337–348. http://dx.doi.org/10.1007/s10974-011-9239-8

Gordon, A.M., E. Homsher, and M. Regnier. 2000. Regulation of contraction in striated muscle. *Physiol. Rev.* 80:853–924.

Grynkiewicz, G., M. Poenie, and R.Y. Tsien. 1985. A new generation of Ca^{2+} indicators with greatly improved fluorescence properties. *J. Biol. Chem.* 260:3440–3450.

Hollingworth, S., M. Zhao, and S.M. Baylor. 1996. The amplitude and time course of the myoplasmic free [Ca^{2+}] transient in fast-twitch fibers of mouse muscle. *J. Gen. Physiol.* 108:455–469. http://dx.doi.org/10.1085/jgp.108.5.455

Hollingworth, S., M.M. Kim, and S.M. Baylor. 2012. Measurement and simulation of myoplasmic calcium transients in mouse slow-twitch muscle fibres. *J. Physiol.* 590:575–594. http://dx.doi.org/10.1113/jphysiol.2011.220780

Klug, G.A., B.R. Botterman, and J.T. Stull. 1982. The effect of low frequency stimulation on myosin light chain phosphorylation in skeletal muscle. *J. Biol. Chem.* 257:4688–4690.

Konishi, M., S. Hollingworth, A.B. Harkins, and S.M. Baylor. 1991. Myoplasmic calcium transients in intact frog skeletal muscle fibers monitored with the fluorescent indicator furaptra. *J. Gen. Physiol.* 97:271–301. http://dx.doi.org/10.1085/jgp.97.2.271

Konishi, M., N. Suda, and S. Kurihara. 1993. Fluorescence signals from the Mg^{2+}/Ca^{2+} indicator furaptra in frog skeletal muscle fibers. *Biophys. J.* 64:223–239. http://dx.doi.org/10.1016/S0006-3495(93)81359-6

Laemmli, U.K. 1970. Cleavage of structural proteins during the assembly of the head of bacteriophage T4. *Nature.* 227:680–685. http://dx.doi.org/10.1038/227680a0

Lee, R.S., S.B. Tikunova, K.P. Kline, H.G. Zot, J.E. Hasbun, N.V. Minh, D.R. Swartz, J.A. Rall, and J.P. Davis. 2010. Effect of Ca^{2+} binding properties of troponin C on rate of skeletal muscle force redevelopment. *Am. J. Physiol. Cell Physiol.* 299:C1091–C1099. http://dx.doi.org/10.1152/ajpcell.00491.2009

Lehrer, S.S. 2011. The 3-state model of muscle regulation revisited: is a fourth state involved? *J. Muscle Res. Cell Motil.* 32:203–208. http://dx.doi.org/10.1007/s10974-011-9263-8

MacIntosh, B.R., M.J. Smith, and D.E. Rassier. 2008. Staircase but not posttetanic potentiation in rat muscle after spinal cord hemisection. *Muscle Nerve.* 38:1455–1465. http://dx.doi.org/10.1002/mus.21096

Manning, D.R., and J.T. Stull. 1982. Myosin light chain phosphorylation-dephosphorylation in mammalian skeletal muscle. *Am. J. Physiol.* 242:C234–C241.

Månsson, A., J. Mörner, and K.A. Edman. 1989. Effects of amrinone on twitch, tetanus and shortening kinetics in mammalian skeletal muscle. *Acta Physiol. Scand.* 136:37–45. http://dx.doi.org/10.1111/j.1748-1716.1989.tb08627.x

Maytum, R., S.S. Lehrer, and M.A. Geeves. 1999. Cooperativity and switching within the three-state model of muscle regulation. *Biochemistry.* 38:1102–1110. http://dx.doi.org/10.1021/bi981603e

McKillop, D.F., and M.A. Geeves. 1993. Regulation of the interaction between actin and myosin subfragment 1: evidence for three states of the thin filament. *Biophys. J.* 65:693–701. http://dx.doi.org/10.1016/S0006-3495(93)81110-X

Moore, R.L., and J.T. Stull. 1984. Myosin light chain phosphorylation in fast and slow skeletal muscles in situ. *Am. J. Physiol.* 247:C462–C471.

Moore, R.L., B.M. Palmer, S.L. Williams, H. Tanabe, R.W. Grange, and M.E. Houston. 1990. Effect of temperature on myosin phosphorylation in mouse skeletal muscle. *Am. J. Physiol.* 259:C432–C438.

Morgan, D.L., D.R. Claflin, and F.J. Julian. 1997. The relationship between tension and slowly varying intracellular calcium concentration in intact frog skeletal muscle. *J. Physiol.* 500:177–192.

Persechini, A., J.T. Stull, and R. Cooke. 1985. The effect of myosin phosphorylation on the contractile properties of skinned rabbit skeletal muscle fibers. *J. Biol. Chem.* 260:7951–7954.

Raju, B., E. Murphy, L.A. Levy, R.D. Hall, and R.E. London. 1989. A fluorescent indicator for measuring cytosolic free magnesium. *Am. J. Physiol.* 256:C540–C548.

Rassier, D.E., L.A. Tubman, and B.R. MacIntosh. 1999. Staircase in mammalian muscle without light chain phosphorylation. *Braz. J. Med. Biol. Res.* 32:121–129. http://dx.doi.org/10.1590/S0100-879X1999000100018

Robertson, S.P., J.D. Johnson, and J.D. Potter. 1981. The time-course of Ca^{2+} exchange with calmodulin, troponin, parvalbumin, and myosin in response to transient increases in Ca^{2+}. *Biophys. J.* 34:559–569. http://dx.doi.org/10.1016/S0006-3495(81)84868-0

Ryder, J.W., K.S. Lau, K.E. Kamm, and J.T. Stull. 2007. Enhanced skeletal muscle contraction with myosin light chain phosphorylation by a calmodulin-sensing kinase. *J. Biol. Chem.* 282:20447–20454. http://dx.doi.org/10.1074/jbc.M702927200

Schiaffino, S., and C. Reggiani. 2011. Fiber types in mammalian skeletal muscles. *Physiol. Rev.* 91:1447–1531. http://dx.doi.org/10.1152/physrev.00031.2010

Smith, I.C., J. Huang, J. Quadrilatero, A.R. Tupling, and R. Vandenboom. 2010. Posttetanic potentiation in mdx muscle. *J. Muscle Res. Cell Motil.* 31:267–277. http://dx.doi.org/10.1007/s10974-010-9229-2

Stull, J.T., K.E. Kamm, and R. Vandenboom. 2011. Myosin light chain kinase and the role of myosin light chain phosphorylation in skeletal muscle. *Arch. Biochem. Biophys.* 510:120–128. http://dx.doi.org/10.1016/j.abb.2011.01.017

Sweeney, H.L., and M.J. Kushmerick. 1985. Myosin phosphorylation in permeabilized rabbit psoas fibers. *Am. J. Physiol.* 249:C362–C365.

Sweeney, H.L., and J.T. Stull. 1986. Phosphorylation of myosin in permeabilized mammalian cardiac and skeletal muscle cells. *Am. J. Physiol.* 250:C657–C660.

Tubman, L.A., D.E. Rassier, and B.R. MacIntosh. 1996. Absence of myosin light chain phosphorylation and twitch potentiation in atrophied skeletal muscle. *Can. J. Physiol. Pharmacol.* 74:723–728. http://dx.doi.org/10.1139/y96-065

Tubman, L.A., D.E. Rassier, and B.R. MacIntosh. 1997. Attenuation of myosin light chain phosphorylation and posttetanic potentiation in atrophied skeletal muscle. *Pflugers Arch.* 434:848–851. http://dx.doi.org/10.1007/s004240050474

Vandenboom, R., J. Xeni, N.M. Bestic, and M.E. Houston. 1997. Increased force development rates of fatigued mouse skeletal muscle are graded to myosin light chain phosphate content. *Am. J. Physiol.* 272:R1980–R1984.

Vandenboom, R., D.R. Claflin, and F.J. Julian. 1998. Effects of rapid shortening on rate of force regeneration and myoplasmic $[Ca^{2+}]$ in intact frog skeletal muscle fibres. *J. Physiol.* 511:171–180. http://dx.doi.org/10.1111/j.1469-7793.1998.171bi.x

Wang, Y., and W.G. Kerrick. 2002. The off rate of Ca^{2+} from troponin C is regulated by force-generating cross bridges in skeletal muscle. *J. Appl. Physiol.* 92:2409–2418.

Westerblad, H., and D.G. Allen. 1993. The contribution of $[Ca^{2+}]_i$ to the slowing of relaxation in fatigued single fibres from mouse skeletal muscle. *J. Physiol.* 468:729–740.

Xeni, J., W.B. Gittings, D. Caterini, J. Huang, M.E. Houston, R.W. Grange, and R. Vandenboom. 2011. Myosin light-chain phosphorylation and potentiation of dynamic function in mouse fast muscle. *Pflugers Arch.* 462:349–358. http://dx.doi.org/10.1007/s00424-011-0965-y

Zhao, F.Q., and R. Craig. 2003. Ca^{2+} causes release of myosin heads from the thick filament surface on the milliseconds time scale. *J. Mol. Biol.* 327:145–158. http://dx.doi.org/10.1016/S0022-2836(03)00098-6

Zhao, F.Q., and R. Craig. 2008. Millisecond time-resolved changes occurring in Ca^{2+}-regulated myosin filaments upon relaxation. *J. Mol. Biol.* 381:256–260. http://dx.doi.org/10.1016/j.jmb.2008.06.032

Zhao, M., S. Hollingworth, and S.M. Baylor. 1997. AM-loading of fluorescent Ca^{2+} indicators into intact single fibers of frog muscle. *Biophys. J.* 72:2736–2747. http://dx.doi.org/10.1016/S0006-3495(97)78916-1

Zhi, G., J.W. Ryder, J. Huang, P. Ding, Y. Chen, Y. Zhao, K.E. Kamm, and J.T. Stull. 2005. Myosin light chain kinase and myosin phosphorylation effect frequency-dependent potentiation of skeletal muscle contraction. *Proc. Natl. Acad. Sci. USA.* 102:17519–17524. http://dx.doi.org/10.1073/pnas.0506846102